RESEARCH ARTICLE | MARCH 24 2026

Spectrally tunable singular phase at normal incidence in nanophotonic cavities

Kandammathe Valiyaveedu Sreekanth ; Sambhu Jana ; Liang Xinan ; Lin Ronghui ; Jinghua Teng

APL Engineering Physics 1, 016105 (2026)
https://doi.org/10.1063/5.0310658

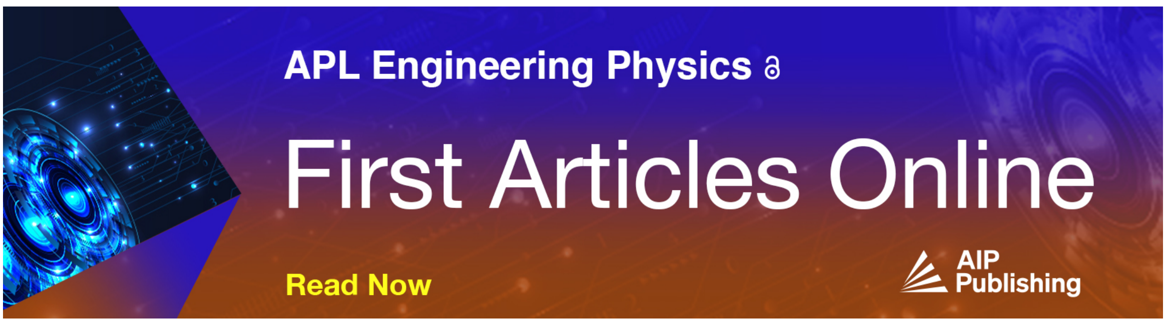

APL Engineering Physics ARTICLE pubs.aip.org/aip/aep

Spectrally tunable singular phase at normal incidence in nanophotonic cavities

Cite as: APL Eng. Phys. 1, 016105 (2026); doi: 10.1063/5.0310658
Submitted: 4 November 2025 • Accepted: 12 February 2026 •
Published Online: 24 March 2026

Kandammathe Valiyaveedu Sreekanth,[1,2,a)] Sambhu Jana,[3,4] Liang Xinan,[1,2] Lin Ronghui,[1,2] and Jinghua Teng[1,2,a)]

AFFILIATIONS

[1] Institute of Materials Research and Engineering, Agency for Science, Technology and Research (A*STAR), 2 Fusionopolis Way, Innovis #08-03, Singapore 138634, Republic of Singapore
[2] National Semiconductor Translation and Innovation Centre (NSTIC), 1 Fusionopolis Way, #19-10 Connexis North, Singapore 138632, Republic of Singapore
[3] Division of Physics and Applied Physics, School of Physical and Mathematical Sciences. Nanyang Technological University, Singapore 637371, Republic of Singapore
[4] Centre for Disruptive Photonic Technologies, The Photonics Institute, Nanyang Technological University, Singapore 637371, Republic of Singapore

[a)] **Authors to whom correspondence should be addressed:** sreekanth@a-star.edu.sg and jh-teng@a-star.edu.sg

ABSTRACT

The concept of singular phases at the point of darkness has been extensively studied using various optical systems, such as metamaterials and thin-film cavities, mainly for refractive index sensing. However, these systems typically work at an oblique angle of incidence. Achieving a singular phase at normal incidence is vital for practical sensing and flat-optics applications, but it remains challenging. Here, we demonstrate the singular phase at normal incidence using a grating-coupled thin-film cavity that functions at optical wavelengths. By optimizing the structural parameters of the grating and thin-film cavity, we achieve zero reflection with an abrupt phase shift at the polarization-dependent resonance of the grating. In addition, we introduce a spectrally tunable singular phase at normal incidence by integrating a phase change material (PCM) into the cavity. Using a lossless PCM, such as Sb_2S_3, we achieve a phase singularity with continuous spectral tunability up to 203 nm by altering its phase from amorphous to crystalline, a key feature for phase engineering in flat optics.

In recent years, the concept of a singular phase has gained attention as a promising approach for ultrasensitive refractive sensing.[1] This effect has been widely studied in various optical systems, including metamaterials[1–5] and Fabry–Pérot (F–P) cavities,[6–14] where light reflection drops to zero at certain incident angles and polarization states. In addition, multiple singular phases and active control over them have been achieved by combining high-refractive-index two-dimensional materials with F–P cavities[15] and by applying a thin organic molecule film on a Si substrate,[16] respectively. However, all reported systems exhibit a singular phase only under specific conditions, mainly at higher incident angles, since zero reflection at the cavity resonance can be achieved only at high incident angles. Recently, a Tamm cavity was introduced to produce a dual-singular phase at a single lower incident angle.[17] It enables the p- and s-polarizations, each exhibiting zero reflection at slightly different wavelengths at the same incident angle, thanks to the Tamm resonance. For practical sensing and flat-optics applications, achieving a singular phase at normal incidence is essential. A recent theoretical study proposed a grating-modulated F–P cavity that generates a singular phase at the hybrid mode by coupling between the F–P cavity and the grating resonances at a normal incidence.[18]

Phase change materials (PCMs) are used to create a controllable singular phase by incorporating chalcogenide PCMs into F–P cavities.[19–24] This enables continuous tuning by changing the PCM's refractive index through the structural phase change from amorphous to crystalline. However, the magnitude of the singular phase gradually decreases due to linewidth broadening in the cavity resonance and the inability to achieve zero reflection in the crystalline PCM state. Recently, a lossless PCM-based Tamm cavity was developed to allow spectrally tunable dual singular phases at a lower incident angle.[17] In addition, achieving spectrally tunable singular phases at normal incidence benefits phase engineering in flat optics and improves sensor detection limits, as phase singularities at different wavelengths can be used for sensing.

In this work, we experimentally demonstrate the singular phase at normal incidence using a visible-wavelength, grating-coupled thin-film cavity. We achieve the singular phase at the polarization-dependent resonance wavelength of a one-dimensional (1D) diffraction grating by optimizing both the thin-film cavity and the grating's structural parameters. Moreover, we introduce a lossless PCM-integrated cavity that showcases a spectrally tunable singular phase at a normal incidence, with large spectral tunability in the near-infrared wavelengths and equal phase changes in both PCM states.

Figure 1(a) illustrates the proposed grating-coupled thin-film cavity designed to generate a singular phase at normal incidence. The structure includes a top Au 1D grating and a bottom Ag layer that serves as a cavity mirror. An ultrathin Ge layer is deposited on the Ag film, which is then topped with an optically thick, transparent SiO_2 cavity layer. Previously, we proposed a similar thin-film cavity without 1D grating to achieve a singular phase at an oblique incidence; in that case, the parameters of the ultrathin, highly absorbing layer and the top metal were essential.[6,25] Since the cavity itself is polarization-independent at a normal incidence, 1D diffraction grating on the top Au layer introduces polarization dependence and facilitates phase difference extraction at the grating resonance. The interaction occurs through momentum matching and near-field overlap between the grating-supported plasmonic modes and the optical modes confined within the cavity.[26,27] This coupling is polarization-sensitive, with a stronger response for transverse magnetic (TM) polarization, and it is dispersive along the grating direction. To attain the singular phase at the darkness point, optimizing cavity and grating parameters is key. The optimal thicknesses are 35 nm for Au, 810 nm for SiO_2, 8 nm for Ge, and 100 nm for Ag. The 1D grating has a linewidth of 100 nm, a period of 400 nm, and an etching depth of 25 nm.

Commercial FDTD simulation software (Ansys Lumerical FDTD) was used to compute the singular phase. Boundary conditions were set as periodic along the x axis and perfectly matched layers (PML) along the z axis. The materials' optical constants, measured experimentally, were incorporated into the simulation (see the supplementary material, Fig. S1). Figure 1(b) presents the reflectance of the grating-coupled cavity at normal incidence for TM and TE polarizations, compared to the cavity alone. The TE reflectance (electric field transverse to the plane of incidence) behaves similarly to that of the cavity alone. However, a sharp zero-reflection dip occurs at 745 nm for TM polarization (magnetic field transverse to the plane of incidence), indicating the excitation of surface plasmon polaritons (SPPs) in the grating-coupled cavity modulated by plasmon-cavity hybridization. The near-field enhancement observed supports this, confirming SPP excitation at 745 nm for TM polarization (see the supplementary material, Fig. S2). The mode at 570 nm corresponds to the grating's surface plasmon resonance, while the mode at 870 nm arises from hybridization between the cavity mode and the grating's SPP. Plasmon-cavity hybridization occurs

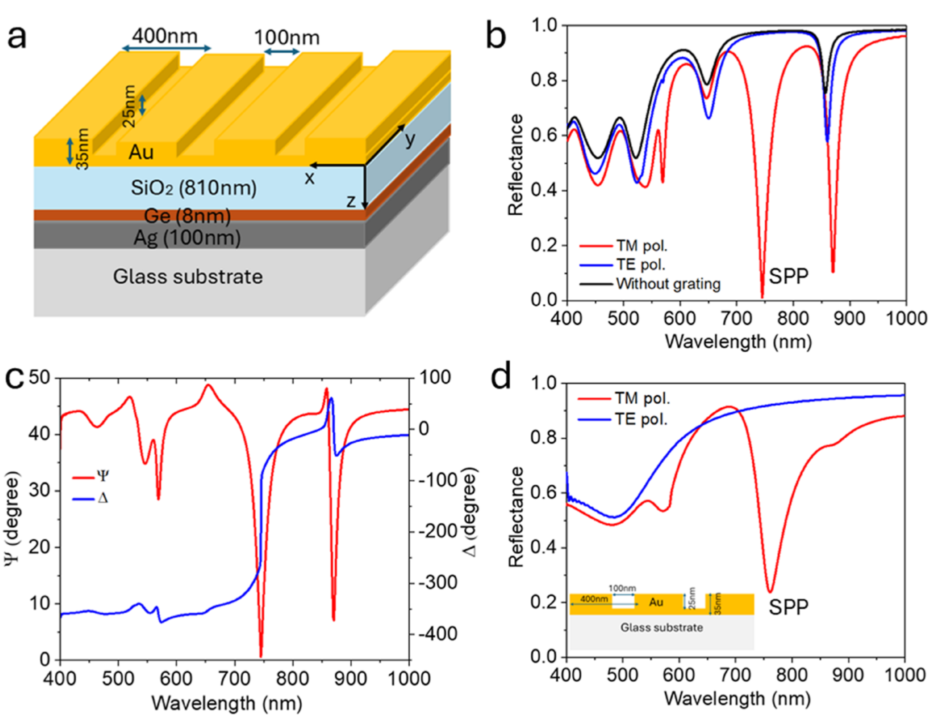

FIG. 1. (a) Schematic of the designed grating-coupled thin film cavity. (b) Calculated reflection spectrum of the cavity alone and the grating-coupled cavity for TM and TE polarizations at a normal incidence. (c) Calculated reflection amplitude (Ψ) and phase difference (Δ) spectra of the grating-coupled cavity. (d) Reflection spectrum of the 1D grating alone for TM and TE polarizations.

when the following conditions are satisfied:[26,27] (i) the energy can be exchanged coherently between the plasmonic and photonic modes when their spectral resonances overlap and in-plane momentum is matched. (ii) The strong evanescent field generated by the grating penetrates the cavity, and the cavity mode exhibits a finite electric field at the metal interface. This means that stronger near-field overlap leads to stronger hybridization. Because of the significant difference in intensity between TM and TE polarizations at 745 nm, a point of zero reflection ($\Psi = 0$) with a sudden phase change can occur. To illustrate this, we calculated the reflection amplitude (Ψ) and phase difference (Δ) between TM and TE polarizations from

$$\rho = \frac{r_{TM}}{r_{TE}} = \tan \Psi e^{i\Delta}. \tag{1}$$

Figure 1(c) shows the spectra of Ψ and Δ at a normal incidence, revealing a singular phase at 745 nm. However, a small phase change is seen at 870 nm because the zero-reflection point is not reached. As shown in Fig. 1(d), the reflectance of a 1D grating alone for TM and TE polarizations exhibits three plasmonic modes, with a pronounced dip at the SPP resonance. Still, zero reflection with a singular phase cannot be attained at the SPP resonance, even by tuning the grating's structural parameters (see the supplementary material, Fig. S3). This demonstrates that the grating-coupled cavity system is essential to realize a singular phase at a normal incidence.

The grating-coupled cavity design was fabricated via physical vapor deposition and focused ion beam (FIB) techniques. First, a 100 nm thick Ag film was deposited on cleaned quartz substrates, followed by 8 nm of Ge, 810 nm of SiO_2, and 35 nm of Au. Thin films of Ag, Ge, and Au were deposited by thermal evaporation (Oerlikon Leybold vacuum), while a thick SiO_2 layer was deposited by ion-assisted deposition (Oxford Optofab3000). Next, an FIB system (FEI Helios NanoLab 600) was used to carve a 1D grating into the Au layer. Using a beam current ≤18 pA and varying exposure doses, we etched varying depths in the Au film. As shown in Fig. 2(a), 1D grating with a period of about 400 nm and an etch width of around 100 nm was patterned over a 25 × 25 μm^2 area. Normal-incidence reflectance measurements were performed with a microspectrophotometer (CRAIC QDI-2010), covering a 25 × 25 μm^2 sample area. The reflectance spectra for TM and TE polarizations are shown in Fig. 2(b), revealing that SPP excitation occurs at around 735 nm for TM polarization, consistent with the simulation. However, zero reflection is not achieved because accurately controlling the etching depth with FIB is challenging, which accounts for the discrepancy between the simulation and experimental results. Moreover, the prominent peak-to-dip features observed near the resonance could be attributed to the quality of the fabricated grating, as the surface roughness of the grating, created on a thin metal film using FIB, is likely quite high. Note that the grating parameters, especially etching depth and metal thickness, are crucial for reaching zero reflection at the SPP resonance (see the supplementary material, Fig. S4).

We then used phase-shift Michelson microscopic interferometry[28,29] to measure the phase change around the resonance. As shown in Fig. 3(a), the microscopic interferometer consists of a supercontinuum fiber laser source (NKT SuperK Extreme equipped with a tunable filter, NKT SuperK SELECT), a beam splitter, two long-working-distance microscope objectives, a tube lens, a mirror mounted on a high-precision piezo stage (PI P-620Z), and a monochrome camera (Thorlabs, CS2100M-USB). A collimated laser beam is divided into two arms via a beam splitter: one arm illuminates the sample surface and reflects as the signal beam, while the other is directed onto the mirror mounted on the piezo stage and reflects as the reference beam. After recombination at the beam splitter, the signal and reference beams interfere, forming an interferogram on the camera plane. The microscope objectives and tube lens ensure the interferogram captured by the camera is a sample-image interferogram. By incrementally shifting the mirror in steps of 1/8 wavelength using the piezo stage, five interferograms—denoted as I_1, I_2, I_3, I_4, and I_5—are captured by the camera. The phase modulation φ (x, y) is then retrieved using the following formula:

$$\varphi(x, y) = \arctan \left[\frac{2(I_2 - I_4)}{2I_3 - I_5 - I_1}\right]. \tag{2}$$

A sine–cosine filter is used to reduce high-frequency noise. The phase data are then unwrapped to create a phase map that covers a specific wavelength range. This map, shown in Fig. 3(b), spans 700–800 nm in 1 nm steps. A notable phase jump near 735 nm is caused by differences in reflection amplitudes between TM and TE polarizations. While these data support the simulation results, achieving zero reflection is crucial for obtaining a singular phase at resonance. We further confirm through numerical analysis that the sensing performance of the proposed grating-coupled cavity shows

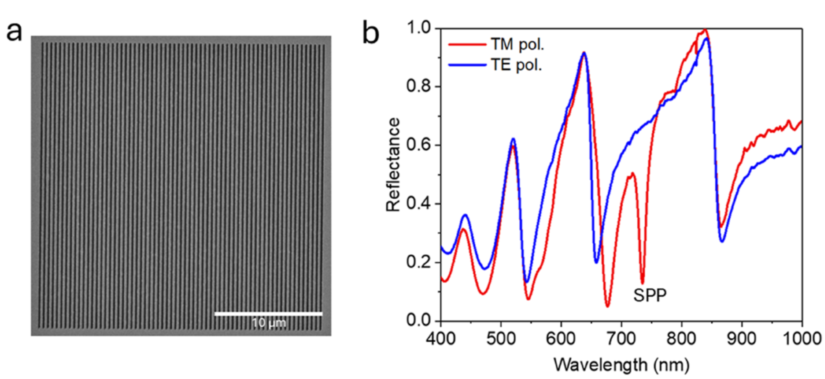

FIG. 2. (a) Scanning electron microscope image of a patterned one-dimensional grating covering a 25 × 25 μm^2 area, with a 400 nm period and an etching width of 100 nm. (b) The measured reflectance spectrum of the grating-coupled thin film cavity for TM and TE polarizations.

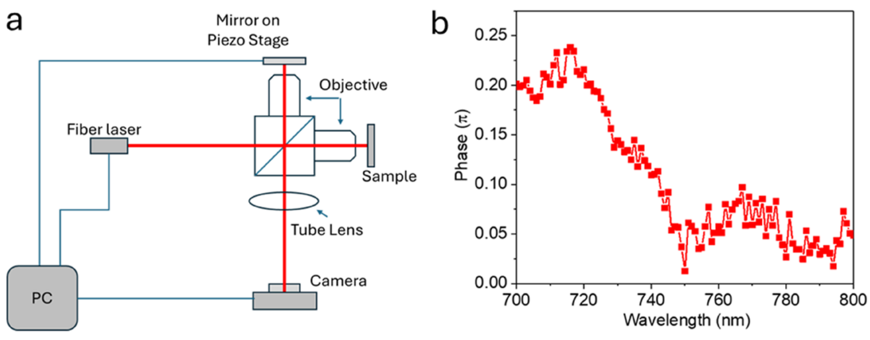

FIG. 3. (a) Schematic of a phase-shift Michelson microscopic interferometry experimental setup. (b) The measured phase spectrum of the grating-coupled thin film cavity.

bulk refractive-index sensitivity comparable with that of cavity-based sensing systems operating at an oblique incidence[9,30] (see the supplementary material, Fig. S5).

To replicate the same phase change at the singular phase wavelengths across a spectral band, a continuously tunable zero-reflection resonance with matching linewidth is required. We introduce a PCM-based tunable grating-coupled cavity for spectrally adjustable singular phase at a normal incidence. Because a lossless cavity layer is necessary, the SiO_2 layer is replaced with a phase change material such as Sb_2S_3, which remains lossless in both amorphous (Amp) and crystalline (Cry) phases within the near-infrared range (see the supplementary material, Fig. S6). As shown in Fig. 4(a), the optimal thicknesses for Sb_2S_3 and Au are 320 and 58 nm, respectively. Other layer thicknesses remain the same as in Fig. 1(a). The designed 1D grating has a period of 420 nm, an etch width of 90 nm, and an etch depth of 58 nm. The reflection spectra for TM and TE polarization in both Amp and Cry phases of Sb_2S_3 are shown in Fig. 4(b). A sharp zero-reflection resonance occurs for TM polarization at 1000 nm in the Amp phase. Switching to the Cry phase shifts this resonance to 1203 nm without affecting the linewidth or the zero reflection, resulting in a 203 nm spectral shift. The Ψ and Δ spectra for the Amp and Cry Sb_2S_3-based cavities are shown in Figs. 4(c) and 4(d), demonstrating the spectral tunability of the singular phase at the darkness point. In addition, this design allows multi-state forward tuning of the singular phase, potentially benefiting applications in flat optics and multispectral spatial light modulators.[29] Moreover, laser interference lithography[31–33] can be used to fabricate large-area 1D periodic gratings, which is vital for the development of scalable singular-phase thin-film coating.

In conclusion, we demonstrated a singular phase at normal incidence using a grating-coupled thin-film cavity. By carefully designing the grating and cavity parameters, we achieved a singular

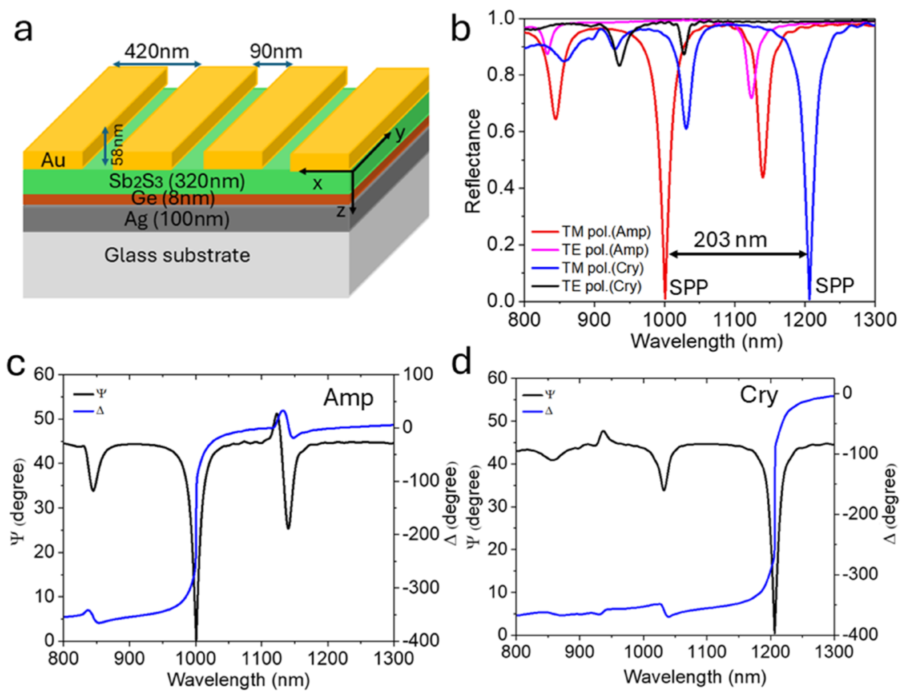

FIG. 4. (a) Schematic of the PCM-based tunable grating-coupled cavity. (b) Calculated polarized reflection spectrum (TM and TE) of the grating-coupled cavity at normal incidence for amorphous and crystalline phases of Sb_2S_3. Calculated reflection amplitude (Ψ) and phase difference (Δ) spectra of the grating-coupled cavity when the phase of Sb_2S_3 is in (c) amorphous and (d) crystalline states.

phase at the 1D grating's SPP resonance wavelength. We employed a phase-shift Michelson interferometer to detect the phase jump at resonance, which could serve as a valuable tool for sensing applications. Importantly, this scheme can be integrated with imaging technology to develop high-throughput sensors, since phase-shift data are easier to collect than angle- or wavelength-shift data. In addition, a spectrally tunable singular phase spanning 203 nm has been numerically demonstrated using a PCM-based grating-coupled thin-film cavity.

The supplementary material provides additional experimental and simulation results.

J.T. acknowledges the support from the Agency for Science, Technology and Research (A*STAR) under MTC Programmatic (Grant No. M22L1b0110), the National Research Foundation, Singapore under NRF-CRP (Grant No. NRF-CRP26-2021-0004), and the National Semiconductor Translation and Innovation Centre (NSTIC).

AUTHOR DECLARATIONS

Conflict of Interest

The authors have no conflicts to disclose.

Author Contributions

Kandammathe Valiyaveedu Sreekanth: Conceptualization (equal); Data curation (equal); Formal analysis (equal); Investigation (equal); Methodology (equal); Writing – original draft (equal). **Sambhu Jana**: Data curation (equal); Investigation (equal). **Liang Xinan**: Data curation (equal); Formal analysis (equal); Investigation (equal). **Lin Ronghui**: Data curation (equal); Formal analysis (equal). **Jinghua Teng**: Funding acquisition (equal); Project administration (equal); Supervision (equal); Writing – review & editing (equal).

DATA AVAILABILITY

The data that support the findings of this study are available from the corresponding author upon reasonable request.

REFERENCES

[1] V. G. Kravets, F. Schedin, R. Jalil, L. Britnell, R. V. Gorbachev, D. Ansell, B. Thackray, K. S. Novoselov, A. K. Geim, A. V. Kabashin, and A. N. Grigorenko, "Singular phase nano-optics in plasmonic metamaterials for label-free single-molecule detection," Nat. Mater. **12**, 304–309 (2013).

[2] K. V. Sreekanth and T. Yu, "Long range surface plasmons in a symmetric graphene system with anisotropic dielectrics," J. Opt. **15**, 055002 (2013).

[3] L. Malassis, P. Massé, M. Tréguer-Delapierre, S. Mornet, P. Weisbecker, P. Barois, C. R. Simovski, V. G. Kravets, and A. N. Grigorenko, "Topological darkness in self-assembled plasmonic metamaterials," Adv. Mater. **26**, 324–330 (2014).

[4] A. I. Aristov, M. Manousidaki, A. Danilov, K. Terzaki, C. Fotakis, M. Farsari, and A. V. Kabashin, "3D plasmonic crystal metamaterials for ultra-sensitive biosensing," Sci. Rep. **6**, 25380 (2016).

[5] A. Berkhout and A. F. Koenderink, "Perfect absorption and phase singularities in plasmon antenna array etalons," ACS Photonics **6**, 2917–2925 (2019).

[6] K. V. Sreekanth, S. Sreejith, S. Han, A. Mishra, X. Chen, H. Sun, C. T. Lim, and R. Singh, "Biosensing with the singular phase of an ultrathin metal-dielectric nanophotonic cavity," Nat. Commun. **9**, 369 (2018).

[7] E. Cusworth, V. G. Kravets, and A. N. Grigorenko, "Topological darkness in optical heterostructures: Prediction and confirmation," ACS Photonics **10**, 3715–3722 (2023).

[8] M. Liu, C. Zhao, Y. Zeng, Y. Chen, C. Zhao, and C.-W. Qiu, "Evolution and nonreciprocity of loss-induced topological phase singularity pairs," Phys. Rev. Lett. **127**, 266101 (2021).

[9] K. V. Sreekanth, P. Mahalakshmi, S. Han, M. S. Mani Rajan, P. K. Choudhury, and R. Singh, "Brewster mode-enhanced sensing with hyperbolic metamaterial," Adv. Opt. Mater. **7**, 1900680 (2019).

[10] V. Maslova, P. Lebedev, and D. G. Baranov, "Topological phase singularities in light reflection from non-Hermitian uniaxial media," Adv. Opt. Mater. **12**, 2303263 (2024).

[11] X. Li, J. Sheng, Z. Wen, F. Li, X. Huang, M. Zhang, Y. Zhang, D. Cao, X. Shi, F. Liu, and J. Hao, "Double topological phase singularities in highly absorbing ultra-thin film structures for ultrasensitive humidity sensing," Opto-Electron. Adv. **8**, 240091 (2025).

[12] A. R. Rao, K. V. Sreekanth, S. Sreejith, V. Jose, S. Pethe, and R. Singh, "Ultrasensitive detection of heavy metal ions with scalable singular phase thin film optical coatings," Adv. Opt. Mater. **10**, 2102623 (2022).

[13] M. Liu, W. Chen, G. Hu, S. Fan, D. N. Christodoulides, C. Zhao, and C.-W. Qiu, "Spectral phase singularity and topological behavior in perfect absorption," Phys. Rev. B **107**, L241403 (2023).

[14] Y. Zhang, M. T. Phoo, Y. Foo, X. Li, Y. W. Lam, and J. A. Zapien, "Vernier ellipsometry sensing with ultralow limit-of-detection and large dynamic range by tuning of zero-reflection points," Laser Photonics Rev. **18**, 2300801 (2024).

[15] G. Ermolaev, K. Voronin, D. G. Baranov, V. Kravets, G. Tselikov, Y. Stebunov, D. Yakubovsky, S. Novikov, A. Vyshnevyy, A. Mazitov, I. Kruglov *et al.*, "Topological phase singularities in atomically thin high-refractive-index materials," Nat. Commun. **13**, 2049 (2022).

[16] P. A. Thomas, K. S. Menghrajani, and W. L. Barnes, "All-optical control of phase singularities using strong light-matter coupling," Nat. Commun. **13**, 1809 (2022).

[17] K. V. Sreekanth, S. Jana, Q. Y. S. Wu, M. Zhao, R. Singh, and J. Teng, "Dual-phase singularity at a single incident angle with spectral tunability in Tamm cavities," Adv. Mater. **36**, 2408098 (2024).

[18] X. Yue, T. Wang, R. Yan, L. Wang, H. Wang, Y. Wang, J. Zhang, and J. Wang, "High-sensitivity refractive index sensing with the singular phase in normal incidence of an asymmetric Fabry–Perot cavity modulated by grating," Opt Laser. Technol. **157**, 108697 (2023).

[19] K. V. Sreekanth, S. Han, and R. Singh, "$Ge_2Sb_2Te_5$-based tunable perfect absorber cavity with phase singularity at visible frequencies," Adv. Mater. **30**, 1706696 (2018).

[20] K. V. Sreekanth, P. Prabhathan, A. Chaturvedi, Y. Lekina, S. Han, S. Zexiang, E. H. Tong Teo, J. Teng, and R. Singh, "Wide-angle tunable critical coupling in nanophotonic optical coatings with low-loss phase change material," Small **18**, 2202005 (2022).

[21] L. Berguiga, L. Ferrier, C. Jamois, T. Benyattou, X. Letartre, and S. Cueff, "Ultimate phase sensitivity in surface plasmon resonance sensors by tuning critical coupling with phase change materials," Opt. Express **29**, 42162–42175 (2021).

[22] K. V. Sreekanth, C. M. Das, R. Medwal, M. Mishra, Q. Ouyang, R. S. Rawat, K. T. Yong, and R. Singh, "Electrically tunable singular phase and Goos–Hänchen shifts in phase-change-material-based thin-film coatings as optical absorbers," Adv. Mater. **33**, 2006926 (2021).

[23] T. Wang, Q. Liu, T. Li, and Y. Ao, "Scattering singularities in fano-resonant multilayer grating structure with phase-change materials," Opt Laser. Technol. **181**, 111602 (2025).

[24] P. Prabhathan, K. V. Sreekanth, J. Teng, J. H. Ko, Y. J. Yoo, H. H. Jeong, Y. Lee *et al.*, "Roadmap for phase change materials in photonics and beyond," iScience **26**, 107946 (2023).

[25]K. V. Sreekanth, Q. Ouyang, S. Han, K. T. Yong, and R. Singh, "Giant enhancement in Goos-Hänchen shift at the singular phase of a nanophotonic cavity," Appl. Phys. Lett. **112**, 161109 (2018).
[26]S. Chen, G. Li, D. Lei, and K. W. Cheah, "Efficient energy exchange between plasmon and cavity modes via Rabi-analogue splitting in a hybrid plasmonic nanocavity," Nanoscale **5**, 9129–9133 (2013).
[27]D. Chanda, K. Shigeta, T. Truong, E. Lui, A. Mihi, M. Schulmerich, P. V. Braun, R. Bhargava, and J. A. Rogers, "Coupling of plasmonic and optical cavity modes in quasi-three-dimensional plasmonic crystals," Nat. Commun. **2**, 479 (2011).
[28]X. Liang, Y. Yu, X. Xu, Y. H. Fu, V. Valuckas, R. Paniagua-Dominguez, and A. I. Kuznetsov, "Near unity transmission and full phase control with asymmetric Huygens' dielectric metasurfaces for holographic projections," Appl. Opt. **61**, B164–B170 (2022).
[29]S. Mansha, P. Moitra, X. Xu, T. W. W. Mass, R. M. Veetil, X. Liang, S. Q. Li, R. Paniagua-Domínguez, and A. I. Kuznetsov, "High resolution multispectral spatial light modulators based on tunable Fabry-Perot nanocavities," Light: Sci. Appl. **11**, 141 (2022).
[30]K. V. Sreekanth, S. Sreejith, Y. Alapan, M. Sitti, C. T. Lim, and R. Singh, "Microfluidics integrated lithography-free nanophotonic biosensor for the detection of small molecules," Adv. Opt. Mater. **7**, 1801313 (2019).
[31]K. V. Sreekanth and V. M. Murukeshan, "Four beams surface plasmon interference nanoscale lithography for patterning of two-dimensional periodic features," J. Vac. Sci. Technol., B: **28**, 128–130 (2010).
[32]K. V. Sreekanth, V. M. Murukeshan, and J. K. Chua, "A planar layer configuration for surface plasmon interference nanoscale lithography," Appl. Phys. Lett. **93**, 093103 (2008).
[33]R. Liu, L. Cao, D. Liu, L. Wang, S. Saeed, and Z. Wang, "Laser interference lithography—A method for the fabrication of controlled periodic structures," Nanomaterials **13**, 1818 (2023).